PHYSICAL REVIEW D **85,** 095013 (2012)

Phenomenology of light neutralinos in view of recent results at the CERN Large Hadron Collider

A. Bottino,[1] N. Fornengo,[1] and S. Scopel[2]

[1]*Dipartimento di Fisica Teorica, Università di Torino Istituto Nazionale di Fisica Nucleare, Sezione di Torino via P. Giuria 1, I-10125 Torino, Italy*

[2]*Department of Physics, Sogang University Seoul, 121-742, Korea*

(Received 11 January 2012; published 17 May 2012)

We review the status of the phenomenology of light neutralinos in an effective minimal supersymmetric extension of the standard model at the electroweak scale, in light of new results obtained at the CERN Large Hadron Collider. First, we consider the impact of the new data obtained by the CMS Collaboration on the search for the Higgs-boson decay into a tau pair, and by the CMS and LHCb Collaborations on the branching ratio for the decay $B_s \to \mu^+ + \mu^-$. Then, we examine the possible implications of the excess of events found by the ATLAS and CMS Collaborations in a search for a standard-model (SM)-like Higgs boson around a mass of 126 GeV, with a most likely mass region (95% C.L.) restricted to 115.5–131 GeV (global statistical significance about 2.3σ). From the first set of data, we update the lower bound of the neutralino mass to be about 18 GeV. From the second set of measurements, we derive that the excess around $m_H^{\rm SM} = 126$ GeV, which however needs a confirmation by further runs at the LHC, would imply a neutralino in the mass range 18 GeV $\lesssim m_\chi \lesssim$ 38 GeV, with neutralino-nucleon elastic cross sections fitting well the results of the dark matter direct search experiments DAMA/LIBRA and CRESST.

DOI: 10.1103/PhysRevD.85.095013 PACS numbers: 95.35.+d, 11.30.Pb, 12.60.Jv, 95.30.Cq

I. INTRODUCTION

The phenomenology of light neutralinos has been thoroughly discussed in Refs. [1–3] within an effective minimal supersymmetric extension of the standard model (MSSM) at the electroweak scale, where the usual hypothesis of gaugino-mass universality at the scale of grand unified theory of the supergravity models is removed (this model containing neutralinos of mass $m_\chi \lesssim 50$ GeV was dubbed light neutralino model (LNM) [3]); this denomination will also be maintained here.

In Refs. [1–3], it was shown that, in case of R-parity conservation, a light neutralino within the LNM, when it happens to be the lightest supersymmetric particle, constitutes an extremely interesting candidate for the dark matter in the Universe, with direct detection rates accessible to experiments of present generation. More specifically, the following results were obtained: (a) a lower bound on m_χ was derived from the cosmological upper limit on the cold dark matter density; (b) it was shown that the population of light neutralinos fits quite well the DAMA/LIBRA annual modulation results [4,5] over a wide range of m_χ; (c) this same population can explain also results of other direct searches for dark matter (DM) particles which show positive results (CoGeNT [6], CRESST [7]) or possible hints (two-event CDMS [8]) in some restricted intervals of m_χ [3,9,10].

It is obvious that the features of the light neutralino population, and its relevant properties (a–c), drastically depend on the intervening constraints which follow from new experimental results. Of particular impact over the details of the phenomenological aspects of the LNM are the new data obtained at the CERN Large Hadron Collider which, in force of its spectacular performance, is providing a profusion of new information. In this respect, the most relevant results of LHC concern: (i) the lower bounds on the squark and gluino masses, (ii) the correlated bounds on $\tan\beta$ (ratio of the two Higgs vacuum expectation values) and m_A (mass of the CP-odd neutral Higgs boson) derived from the searches for neutral Higgs bosons into a tau-lepton pair, (iii) a new strict upper bound on the branching ratio (BR) for the decay $B_s \to \mu^+ + \mu^-$, (iv) the indication of a possible signal (at a statistical significance of 2.3σ) for a SM-like Higgs boson with a mass of about 126 GeV [11,12].

The impact of item (i) on the LNM was already considered in Ref. [13]. In the present paper, we derive the consequences that the new bounds from searches for neutral Higgs bosons into a tau-lepton pair and from BR($B_s \to \mu^+ + \mu^-$) [items (ii) and (iii) above] have on the phenomenology of the light neutralinos and discuss the implications that a Higgs boson at about 126 GeV [item (iv)] could have, in case this preliminary experimental indication is confirmed in future LHC runs.

II. FEATURES OF THE LIGHT NEUTRALINO MODEL

The LNM is an effective MSSM scheme at the electroweak scale, with the following independent parameters: M_1, M_2, M_3, μ, $\tan\beta$, m_A, $m_{\tilde{q}_{12}}$, $m_{\tilde{t}}$, $m_{\tilde{l}_{12,L}}$, $m_{\tilde{l}_{12,R}}$, $m_{\tilde{\tau}_L}$, $m_{\tilde{\tau}_R}$, and A. We stress that the parameters are defined at the electroweak scale. Notations are as follows: M_1, M_2, and M_3 are the U(1), SU(2), and SU(3) gaugino masses

(these parameters are taken here to be positive), μ is the Higgs mixing mass parameter, $\tan\beta$ the ratio of the two Higgs vacuum expectation values, m_A the mass of the CP-odd neutral Higgs boson, $m_{\tilde{q}_{12}}$ is a squark soft mass common to the squarks of the first two families, $m_{\tilde{t}}$ is the squark soft mass for the third family, $m_{\tilde{l}_{12,L}}$ and $m_{\tilde{l}_{12,R}}$ are the slepton soft mass common to the L, R components of the sleptons of the first two families, $m_{\tilde{\tau}_L}$ and $m_{\tilde{\tau}_R}$ are the slepton soft mass of the L, R components of the slepton of the third family, A is a common dimensionless trilinear parameter for the third family, $A_{\tilde{b}} = A_{\tilde{t}} \equiv A m_{\tilde{t}}$ and $A_{\tilde{\tau}} \equiv A(m_{\tilde{\tau}_L} + m_{\tilde{\tau}_R})/2$ (the trilinear parameters for the other families being set equal to zero). In our model, no gaugino-mass unification at a grand unified scale is assumed, and therefore M_1 can be sizably lighter than M_2. Notice that the present version of the LNM represents an extension of the model discussed in our previous papers [1–3], where a common squark and the slepton soft mass was employed for the 3 families.

The linear superposition of bino $\tilde{B}$, wino $\tilde{W}^{(3)}$, and of the two Higgsino states $\tilde{H}_1^o$, $\tilde{H}_2^o$ which defines the neutralino state of lowest mass m_χ is written here as

$$\chi \equiv a_1\tilde{B} + a_2\tilde{W}^{(3)} + a_3\tilde{H}_1^o + a_4\tilde{H}_2^o. \quad (1)$$

A. The cosmological bound

Since no gaugino-mass unification at a grand unified theory scale is assumed in our LNM (at variance with one of the major assumptions in minimal supergravity), in this model the neutralino mass is not bounded by the lower limit $m_\chi \gtrsim 50$ GeV that is commonly derived in minimal-supergravity schemes from the LEP lower bound on the chargino mass (of about 100 GeV). However, in the case of R-parity conservation the neutralino, when occurs to be the lightest supersymmetric particle, has a lower limit on its mass m_χ which can be derived from the cosmological upper bound on the cold dark matter (CDM) relic abundance $\Omega_{\rm CDM}h^2$. Actually, by employing this procedure, in Ref. [1] a value of 6–7 GeV for the lower limit of m_χ was obtained, and this value was subsequently updated to the value of about 8 GeV in Refs. [3,10] as derived from the experimental data available at that time. Now, with the advent of fresh data from LHC, the lower bound on m_χ has to be redetermined; this will be done in Sec. III A.

To set the general framework, let us recall that the neutralino relic abundance is given by

$$\Omega_\chi h^2 = \frac{x_f}{g_\star(x_f)^{1/2}} \frac{9.9\cdot 10^{-28}\ \mathrm{cm^3\ s^{-1}}}{\langle\widetilde{\sigma_{\rm ann}v}\rangle}, \quad (2)$$

where $\langle\widetilde{\sigma_{\rm ann}v}\rangle \equiv x_f\langle\sigma_{\rm ann}v\rangle_{\rm int}$, $\langle\sigma_{\rm ann}v\rangle_{\rm int}$ being the integral from the present temperature up to the freeze-out temperature T_f of the thermally averaged product of the annihilation cross section times the relative velocity of a pair of neutralinos, x_f is defined as $x_f \equiv m_\chi/T_f$, and $g_\star(x_f)$ denotes the relativistic degrees of freedom of the thermodynamic bath at x_f. For $\langle\widetilde{\sigma_{\rm ann}v}\rangle$, we will use the standard expansion in S and P waves: $\langle\widetilde{\sigma_{\rm ann}v}\rangle \simeq \tilde{a} + \tilde{b}/(2x_f)$. Notice that in the LNM no coannihilation effects are present in the calculation of the relic abundance, due to the large mass splitting between the mass of the neutralino ($m_\chi < 50$ GeV) and those of sfermions and charginos.

The annihilation processes which contribute to $\langle\widetilde{\sigma_{\rm ann}v}\rangle$ at the lowest order are: (i) exchange of a Higgs boson in the s channel, (ii) exchange of a sfermion in the t channel, (iii) exchange of the Z boson in the s channel. In the physical region which we are going to investigate, which entails light values for the masses of supersymmetric Higgs bosons m_h, m_A, m_H (for the lighter CP-even h, the CP-odd A, and the heavier CP-even H, respectively) and a light mass for the stau $\tilde{\tau}$, the contribution of the Z exchange is largely subdominant compared to the first two which can be of the same order, with a dominance of the A-exchange contribution for $m_\chi \lesssim 28$ GeV, and a possible dominance of the $\tilde{\tau}$ exchange afterward (see numerical results in Fig. 3).

In our numerical evaluations, all relevant contributions to the pair annihilation cross section of light neutralinos are included. However, an approximate expression for $\Omega_\chi h^2$, valid for very light neutralinos, proves very useful to obtain an analytic formula for the lower bound for the neutralino mass. Indeed, for $m_\chi \lesssim 28$ GeV when $\langle\widetilde{\sigma_{\rm ann}v}\rangle$ is dominated by the A exchange, $\Omega_\chi h^2$ may be written as [1]

$$\Omega_\chi h^2 \simeq \frac{4.8\cdot 10^{-6}}{\mathrm{GeV}^2} \frac{x_f}{g_\star(x_f)^{1/2}} \frac{1}{a_1^2 a_3^2 \tan^2\beta} \times m_A^4 \frac{[1-(2m_\chi)^2/m_A^2]^2}{m_\chi^2[1-m_b^2/m_\chi^2]^{1/2}} \frac{1}{(1+\epsilon_b)^2}, \quad (3)$$

where ϵ_b is a quantity which enters in the relationship between the b-quark running mass and the corresponding Yukawa coupling (see Ref. [14] and references quoted therein). For neutralino masses in the range $m_\chi =$ (10–20) GeV, $g_\star(x_f)^{1/2} \simeq 2.5$. In deriving this expression, one has taken into account that here the following hierarchy holds for the coefficients a_i of χ [3]:

$$|a_1| > |a_3| \gg |a_2|, |a_4|, \quad (4)$$

whenever $\mu/m_\chi \gtrsim$ a few. In Ref. [3], it is also shown that in this regime

$$a_1^2 a_3^2 \simeq \frac{\sin^2\theta_W m_Z^2 \mu^2}{(\mu^2 + \sin^2\theta_W m_Z^2)^2} \simeq \frac{0.19\mu_{100}^2}{(\mu_{100}^2 + 0.19)^2}, \quad (5)$$

where μ_{100} is μ in units of 100 GeV. From this formula and the LEP lower bound $|\mu| \gtrsim 100$ GeV, we obtain $(a_1^2 a_3^2)_{\rm max} \lesssim 0.13$. This upper bound is essentially equivalent to one which can be derived from the upper bound on

the width for the Z-boson decay into a light neutralino pair: $(a_1^2 a_3^2)_{\max} \lesssim 0.12$ [3].

By imposing that the neutralino relic abundance does not exceed the observed upper bound for CDM, i.e., $\Omega_\chi h^2 \leq (\Omega_{\rm CDM} h^2)_{\max}$, we obtain the following lower bound on the neutralino mass:

$$m_\chi \frac{[1-m_b^2/m_\chi^2]^{1/4}}{[1-(2m_\chi)^2/m_A^2]} \gtrsim 17\ {\rm GeV} \left(\frac{m_A}{90\ {\rm GeV}}\right)^2 \left(\frac{15}{\tan\beta}\right) \times \left(\frac{0.12}{a_1^2 a_3^2}\right)^{(1/2)} \left(\frac{0.12}{(\Omega_{\rm CDM} h^2)_{\max}}\right)^{(1/2)}. \quad (6)$$

Here, we have taken as default value for $(\Omega_{\rm CDM} h^2)_{\max}$ the numerical value which represents the 2σ upper bound to $(\Omega_{\rm CDM} h^2)_{\max}$ derived from the results of Ref. [15]. For ϵ_b, we have used a value which is representative of the typical range obtained numerically in our model: $\epsilon_b = -0.08$.

B. Neutralino-nucleon elastic cross section

We turn now to the evaluation of the neutralino-nucleon elastic cross section $\sigma_{\rm scalar}^{\rm (nucleon)}$, since we are interest here in the comparison of our theoretical evaluations with the most recent data from experiments of direct searches for DM particles.

Notice that we consider here only coherent neutralino-nucleus cross sections, thus spin-dependent couplings are disregarded, and the neutralino-nucleon cross sections are derived from the coherent neutralino-nucleus cross section in the standard way.

The neutralino-nucleon scattering then takes contributions from (h, A, H) Higgs-boson exchange in the t channel and from the squark exchange in the s channel; the A-exchange contribution is suppressed by kinematic effects. In the supersymmetric parameter region considered in the present paper, the contributions from the h and H exchanges are largely dominant over the squark exchange, with a sizable dominance of the h exchange over the H one (a quantitative analysis of this point will be given in Sec. III A in connection with Fig. 4). An approximate expression for $\sigma_{\rm scalar}^{\rm (nucleon)}$, valid at small values of m_χ, is obtained by including only the dominant contribution of the h-boson exchange [3]:

$$\sigma_{\rm scalar}^{\rm (nucleon)} \simeq 9.7 \times 10^{-42}\ {\rm cm}^2 \left(\frac{a_1^2 a_3^2}{0.13}\right) \left(\frac{\tan\beta}{15}\right)^2 \times \left(\frac{90\ {\rm GeV}}{m_h}\right)^4 \left(\frac{g_d}{290\ {\rm MeV}}\right)^2, \quad (7)$$

where

$$g_d \equiv [m_d \langle N|\bar{d}d|N\rangle + m_s \langle N|\bar{s}s|N\rangle + m_b \langle N|\bar{b}b|N\rangle], \quad (8)$$

and the matrix elements $\langle N|\bar{q}q|N\rangle$ denote the scalar quark densities of the d, s, b quarks inside the nucleon.

In Eq. (7), we have used as *reference* value for g_d the value $g_{d,\rm ref} = 290$ MeV employed in our previous papers [2,3]. We recall that this quantity is affected by large uncertainties [16] with $(g_{d,\max}/g_{d,\rm ref})^2 = 3.0$ and $(g_{d,\min}/g_{d,\rm ref})^2 = 0.12$ [2,3]. Notice that these uncertainties still persist [17,18]. Our reference value $g_{d,\rm ref} = 290$ MeV is larger by a factor 1.5 than the central value of Ref. [19], frequently used in the literature.

By employing Eqs. (3) and (7) we find that any neutralino configuration, *whose relic abundance stays in the cosmological range for CDM* [i.e., $(\Omega_{\rm CDM} h^2)_{\min} \leq \Omega_\chi h^2 \leq (\Omega_{\rm CDM} h^2)_{\max}$ with $(\Omega_{\rm CDM} h^2)_{\min} = 0.098$ and $(\Omega_{\rm CDM} h^2)_{\max} = 0.12$] and passes all particle-physics constraints, has an elastic neutralino-nucleon cross section given approximately by [3]

$$\sigma_{\rm scalar}^{\rm (nucleon)} \simeq (2.7 - 3.4) \times 10^{-41}\ {\rm cm}^2 \left(\frac{g_d}{290\ {\rm MeV}}\right)^2 \left(\frac{m_A}{m_h}\right)^4 \times \frac{[1-(2m_\chi)^2/m_A^2]^2}{(m_\chi/(10\ {\rm GeV})^2 [1-m_b^2/m_\chi^2]^{1/2}}. \quad (9)$$

Notice that in the range 90 GeV $\leq m_A \leq$ 120 GeV the maximal values of the ratio m_A/m_h are of order one within a few percent (see left panel of Fig. 2).

We recall that for neutralino configurations whose relic abundance stays below the cosmological range for CDM, i.e., have $\Omega_\chi h^2 < (\Omega_{\rm CDM} h^2)_{\min}$, one has to associate to $\sigma_{\rm scalar}^{\rm (nucleon)}$ a local density rescaled by a factor $\xi = \rho_\chi/\rho_0$, as compared to the total local DM density ρ_χ; ξ is conveniently taken as $\xi = \min\{1, \Omega_\chi h^2/(\Omega_{\rm CDM} h^2)_{\min}\}$ [20].

Furthermore, we note that Eq. (9) is valid when the A-boson exchange is dominating in the neutralino pair annihilation process (in the s channel). As mentioned above, this occurs for $m_\chi \lesssim 28$ GeV. For higher neutralino masses, the actual values of $\sigma_{\rm scalar}^{\rm (nucleon)}$ are somewhat higher than those provided by Eq. (9).

C. Constraints

To single out the physical supersymmetric configurations within our LNM, the following experimental constraints are imposed: accelerators data on supersymmetric and Higgs boson searches at the CERN e^+e^- collider LEP2 [21]; the upper bound on the invisible width for the decay of the Z boson into non-standard-model particles: $\Gamma(Z \to \chi\chi) < 3$ MeV [22,23]; measurements of the $b \to s + \gamma$ decay process [24]: $2.89 \leq {\rm BR}(b \to s\gamma) \cdot 10^4 \leq 4.21$ is employed here (this interval is larger by 25% with respect to the experimental determination [24] in order to take into account theoretical uncertainties in the supersymmetric contributions [25] to the branching ratio of the process (for the standard model calculation, we employ the next-to-next-to-leading-order results from Ref. [26]); the measurements of the muon anomalous magnetic moment $a_\mu \equiv (g_\mu - 2)/2$: for the deviation,

$\Delta a_\mu \equiv a_\mu^{\rm exp} - a_\mu^{\rm the}$, of the experimental world average from the theoretical evaluation within the standard model, we use here the (2σ) range $31 \leq \Delta a_\mu \cdot 10^{11} \leq 479$, derived from the latest experimental [27] and theoretical [28] data (the supersymmetric contributions to the muon anomalous magnetic moment within the MSSM are evaluated here by using the formulas in Ref. [29]); the search for charged Higgs bosons in top quark decay at the Tevatron [30]; the recently improved upper bound (at 95% C.L.) on the branching ratio for the decay $B_s \to \mu^+ + \mu^-$: $\mathrm{BR}(B_s \to \mu^+\mu^-) < 1.08 \times 10^{-8}$ [31] (see also Refs. [32,33]) and the constraints related to $\Delta M_{B,s} \equiv M_{B_s} - M_{\bar{B}_s}$ [34,35].

A further bound, which plays a most relevant role in constraining the supersymmetric parameter space, is represented by the results of searches for Higgs decay into a tau pair. Indeed, colliders have a good sensitivity to the search for decays ($\phi \to b\bar{b}$ or $\phi \to \tau\bar{\tau}$) (where $\phi = h, A, H$) in the regime of small m_A and large $\tan\beta$, because in this region of the supersymmetric parameters the couplings of one of the neutral Higgs bosons to the down fermions are enhanced [36]. This experimental investigation was thoroughly carried out at the Tevatron and is now underway at the LHC. No signal for these decays has been found so far, thus successive measurements have progressively disallowed substantial regions in the supersymmetric parameters space at small m_A and large $\tan\beta$.

However, at present the actual forbidden region is not yet firmly established. The most stringent bounds provided in the $m_A - \tan\beta$ plane are reported by the CMS Collaboration in a preliminary form in Refs. [37,38]. The first report refers to a luminosity of 1.6 fb^{-1}, the second one to a luminosity of 4.6 fb^{-1}. It is worth noting that, in the range 90 GeV $\leq m_\chi \leq$ 120 GeV, the bound on $\tan\beta$ given in the second report is less stringent than the limit given in the first one by a factor of (20–40)%. This circumstance suggests to take the present constraints with much caution. A conservative attitude is also suggested by the considerations put forward in Refs. [39,40] about the actual role of uncertainties in the derivation of the present bounds.

In Fig. 1, which displays the plane $m_A - \tan\beta$, we summarize the present situation as far as the constraints from the collider searches for the neutral Higgs decays into a tau pair are concerned. The dash-dotted line denotes the 95% C.L. upper bound reported in Ref. [38], accounting for a $+1\sigma$ theoretical uncertainty. The dashed line displays the expected upper bound (in case of no positive signal for an integrated luminosity of 3 fb^{-1}) as evaluated in Refs. [39,40]. We do not mean to attribute to this expected bound the meaning of the most realistic upper limit; we just take it as indicative of a conservative estimate of the bound, and thus as a reasonable upper extreme of the physical range to consider in our scan of the parameter space.

Notice that the regime of small $\tan\beta$ values is also compatible with one of the physical regions selected by the branching ratio $\mathrm{BR}(B \to \tau + \nu)$ (see Fig. 16 of Ref. [3]).

Also shown in Fig. 1 are the curves which correspond to a fixed value of m_χ; these are calculated from Eq. (6) by replacing the inequality with an equality symbol and setting, for definiteness, to 1 the two last factors of the right-hand side. Thus, for configurations with different values of $(a_1^2 a_3^2)^{1/2}$, the m_χ value associated to each isomass curve has to be scaled up by the factor $(a_1^2 a_3^2/0.12)^{1/2}$. The features of the scatter plot displayed in Fig. 1 and its implications will be discussed in the next section.

We recall that also the cosmological constraint $\Omega_\chi h^2 \leq (\Omega_{\rm CDM} h^2)_{\rm max}$, discussed in Sec. II A, is implemented in our analysis.

The viability of very light neutralinos in terms of various constraints from collider data, precision observables, and rare meson decays is also considered in Ref. [41]. Perspectives for investigation of these neutralinos at LHC are analyzed in Refs. [42,43] and prospects for a very accurate mass measurement at ILC in Refs. [44].

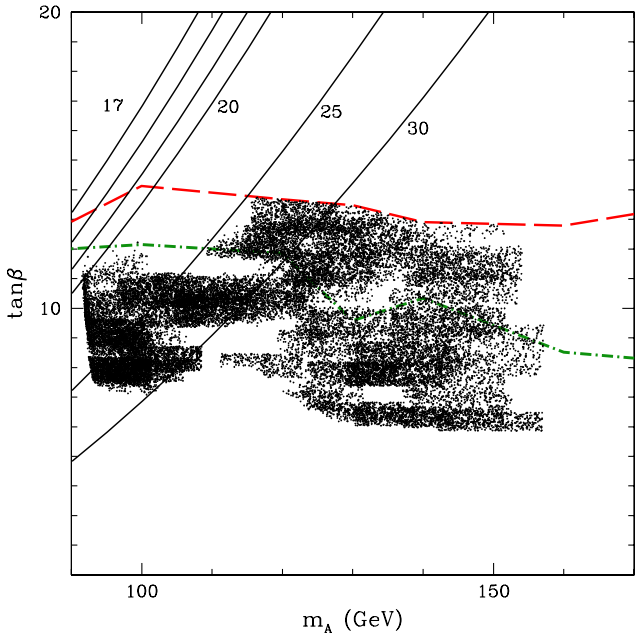

FIG. 1 (color online). Upper bounds in the $m_A - \tan\beta$ plane, derived from searches of the neutral Higgs decays into a tau pair at the LHC. The dash-dotted line denotes the 95% C.L. upper bound reported in Ref. [38]. The dashed line displays the expected upper bound (in case of no positive signal for an integrated luminosity of 3 fb^{-1}) as evaluated in Refs. [39,40]. The scatter plot denotes configurations of the LNM. The solid lines (some of which are labeled by numbers) denote the cosmological bound $\Omega_\chi h^2 \leq (\Omega_{\rm CDM} h^2)_{\rm max}$ for a neutralino whose mass is given by the corresponding number (in units of GeV), as obtained by Eq. (6), with $\epsilon_b = -0.08$ and $(\Omega_{\rm CDM} h^2)_{\rm max} = 0.12$. For any given neutralino mass, the allowed region is above the corresponding line.

III. RESULTS

According to the considerations developed up to now, it is clear that, in order to examine the physical region relevant for light neutralinos with a sizable elastic neutralino-nucleon cross section efficiently, one has to set up a scan of the supersymmetric parameter space focused on low values of M_1, restricted ranges of m_A and μ close to their minimal values as allowed by present experimental lower bounds, and a range of $\tan\beta$ delimited from above by the bounds from the neutral Higgs decays into a tau pair and from $\mathrm{BR}(B_s \to \mu^+ + \mu^-)$. The LEP limits on $\tan\beta$ and m_A are taken into account through the bounds derived from the Higgs-strahlung of the Z boson [21]. The selection of the parameters' ranges has also to allow small values of the tau slepton, to take care of the cosmological bound for neutralinos with $m_\chi \gtrsim 28$ GeV (see previous discussion in Sec. II A).

For these reasons, the scan of the parameter space adopted in the present paper is the following: $1 \leq \tan\beta \leq 15$, $100\ \mathrm{GeV} \leq \mu \leq 200\ \mathrm{GeV}$, $10\ \mathrm{GeV} \leq M_1 \leq 100\ \mathrm{GeV}$, $100\,\mathrm{GeV} \leq M_2 \leq 2000\,\mathrm{GeV}$, $700\,\mathrm{GeV} \leq m_{\tilde{q}_{12}} \leq 2000\,\mathrm{GeV}$, $100\,\mathrm{GeV} \leq m_{\tilde{l}} \leq 1000\,\mathrm{GeV}$, $70\ \mathrm{GeV} \leq m_{\tilde{l}_{12,L}}$, $m_{\tilde{l}_{12,R}}$, $m_{\tilde{\tau}_L}$, $m_{\tilde{\tau}_R} \leq 150\,\mathrm{GeV}$, $90\ \mathrm{GeV} \leq m_A \leq 160\ \mathrm{GeV}$, $0.5 \leq A \leq 3$.

We turn now to the discussion of the physical results as obtained by our numerical scans of the supersymmetric parameter space. First, we analyze the generic population of light neutralinos within the LNM which takes into account all the constraints listed in the previous Sec. II C, then we will discuss the impact of the excess seen by the ATLAS and CMS Collaborations at the LHC.

A. The light neutralino population within the LNM

A first result of our scans is shown in Fig. 1. From the scatter plot displayed here, one sees that the lower bound on the neutralino mass turns out to be about 18 GeV. The depopulation in the domain with $\tan\beta \gtrsim 12$ and $90\ \mathrm{GeV} \lesssim m_A \lesssim 100\ \mathrm{GeV}$ with respect to our previous analyses [3] is due to the new bound $\mathrm{BR}(B_s \to \mu^+\mu^-) < 1.08 \times 10^{-8}$ [31].

In Fig. 2, we display the correlation between m_A and m_h, m_H, because this will be useful for the discussions to follow. From the left panel of Fig. 2, one can derive the values of the ratio m_A/m_h which enters into the approximate estimate of the neutralino-nucleon elastic cross section due to the h-exchange contribution [see Eq. (9)].

Figures 3 and 4 give the size of the various channels contributing to the neutralino pair annihilation and to the neutralino-nucleon elastic cross section, respectively. From Fig. 3, we observe in the neutralino pair annihilation cross section a dominance of the A-exchange contribution for $m_\chi \lesssim 28$ GeV, and a possible dominance of the $\tilde{\tau}$ exchange for larger values of m_χ, as anticipated in Sec. II A (the contribution of the Z exchange is largely subdominant compared to the other two and is not shown). Figure 4 shows that in the direct detection cross section the contributions from the h and H exchanges are largely dominant over the squark exchange, with a sizable dominance of the h exchange over the H one.

The scatter plot for the quantity relevant for the comparison with the direct detection experimental results,

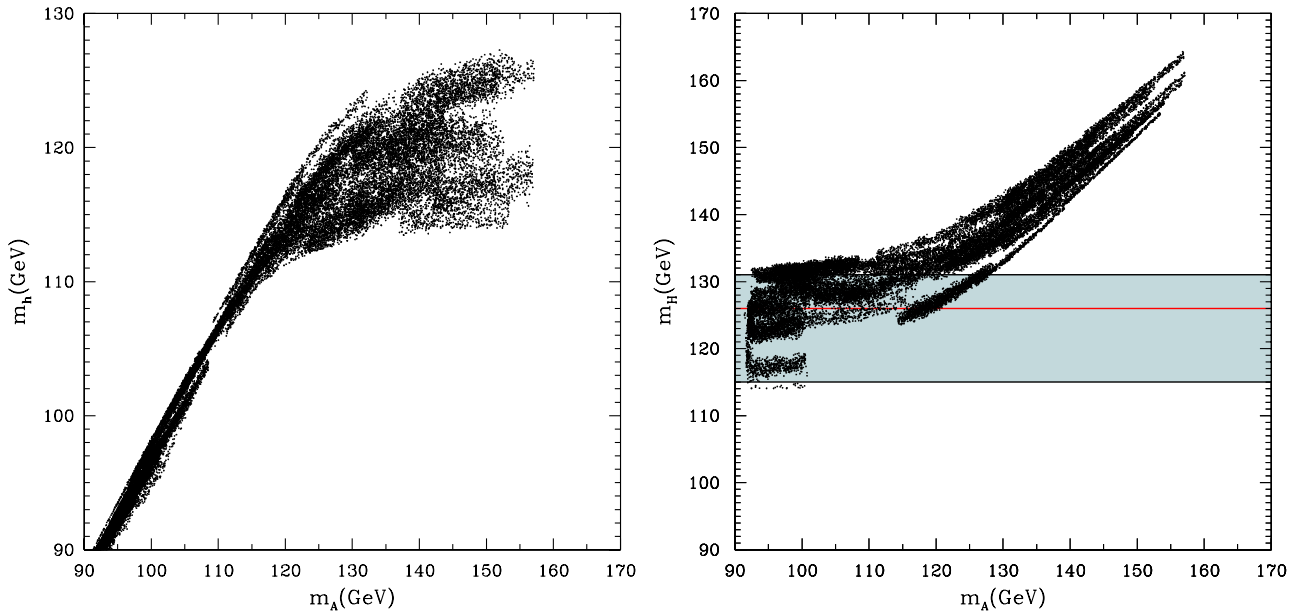

FIG. 2 (color online). Relation among the Higgs masses in the LNM. In the left panel, the correlation between m_h and m_A is shown. In the right panel, the correlation between m_H and m_A is given. The horizontal (red) line and the shaded band around it denote the value of 126 GeV for the Higgs mass (and the 95% C.L. region between 115.5 GeV and 131 GeV) compatible with the excess of events observed by ATLAS [11] and CMS [12].

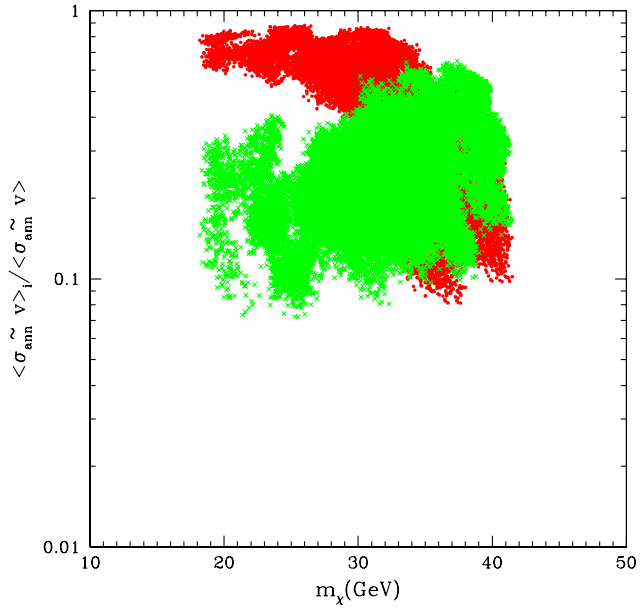

FIG. 3 (color online). Fractional relevance of channels in the neutralino self-annihilation cross section $\langle\widetilde{\sigma_{\rm ann}}v\rangle$ appearing in Eq. (2) as a function of the neutralino mass in the LNM. The (red) points refer to annihilation through A exchange; (green) crosses to annihilation through $\tilde{\tau}$ exchange.

$\xi\sigma^{(\rm nucleon)}_{\rm scalar}$, is displayed in Fig. 5. It is noticeable that our population of light neutralinos fits quite well a region of compatibility of the DAMA/LIBRA data with the CRESST results in the $m_\chi - \xi\sigma^{(\rm nucleon)}_{\rm scalar}$ plane.

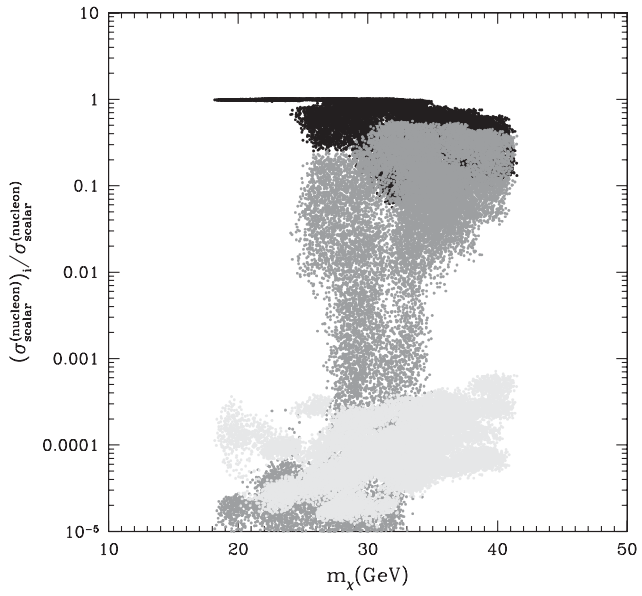

FIG. 4. Fractional relevance of channels in the neutralino-nucleon elastic-scattering cross section as a function of the neutralino mass in the LNM. From darker to lighter points: h exchange, H exchange, $\tilde{q}$ exchange.

Some comments are in order here:

(a) The scatter plot shown in Fig. 5 is obtained with a specific set of values for the hadronic quantities which establish the coupling between the Higgs boson and the nucleon (i.e., $g_d = g_{d,\rm ref} = 290$ MeV). As mentioned in Sec. II B, the quantity g_d suffers from large uncertainties [19], so that the scatter plot of Fig. 5 could actually move upward by a factor 3 or downward by a factor 0.12.

(b) The experimental region of each individual experiment is sizably affected by uncertainties due to the estimate of the quenching factor. In the case of the DAMA/LIBRA experiment, the two regions are illustrative (but not exhaustive) of the large effect introduced by different evaluations of this factor [10].

(c) The position of the experimental regions $m_\chi - \xi\sigma^{(\rm nucleon)}_{\rm scalar}$ strongly depends also on the DM galactic

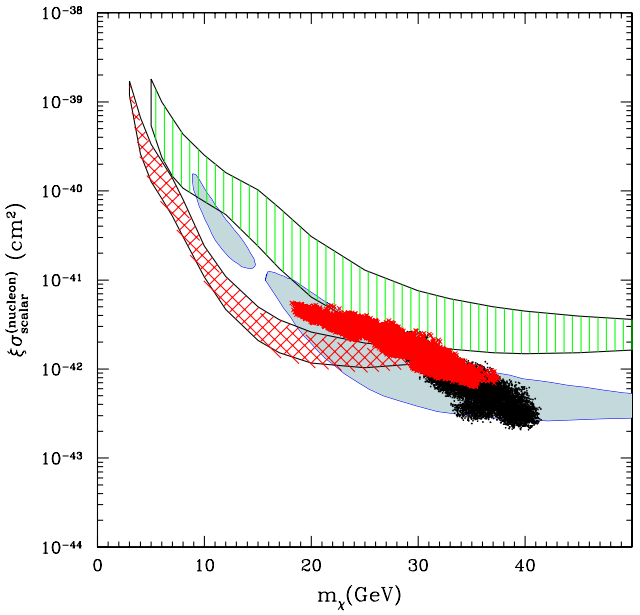

FIG. 5 (color online). Neutralino-nucleon cross section $\xi\sigma^{(\rm nucleon)}_{\rm scalar}$ as a function of the neutralino mass for the LNM scan and for $g_{d,\rm ref} = 290$ MeV. The (red) crosses denote configurations with a heavy Higgs mass in the range compatible with the ATLAS [11] and CMS [12] excess at the LHC. The shaded areas denote the DAMA/LIBRA annual modulation regions: the upper area (vertical shade; green) refers to the case where constant values of 0.3 and 0.09 are taken for the quenching factors of Na and I, respectively [10]; the lower area (cross hatched; red) is obtained by using the energy-dependent Na and I quenching factors as established by the procedure given in Ref. [55]. The gray regions are those compatible with the CRESST excess [7]. In all cases, a possible channeling effect is not included. The halo distribution functions used to extract the experimental regions are given in the text.

distribution function (DF) employed in deriving these regions from the experimental rates. Thus, their location relative to the theoretical scatter plot changes depending on the galactic DM properties [45]. The domains shown in Fig. 5 were obtained by using for the DF the standard isothermal sphere with $\rho_0 = 0.30$ GeV cm^{-3}, $v_0 = 220$ kmsec^{-1}, with $v_{esc} = 650$ kmsec^{-1} for DAMA/LIBRA experiment and $v_{esc} = 544$ kmsec^{-1} for CRESST. The use of a DF with a larger (smaller) value of ρ_0 would move downward (upward) the experimental regions by a factor proportional to ρ_0. Increasing (decreasing) the speeds generically produces a displacement toward lower (higher) masses [45].

In conclusion, by taking into account various sources of uncertainties, mainly the ones mentioned in the two last items, the experimental regions shown in Fig. 5 may change sizably. In the case of the DAMA/LIBRA experiment, the regions which encompass the effects of various uncertainties are plotted in Figs. 1, 2, 3, and 7 of Ref. [10].

Negative results reported by other experiments of DM direct detection [46–48] are in tension with the signals measured by DAMA/LIBRA and CRESST. It should however be noted that a number of questions about various physical and technical features of the specific detectors or of the relevant analyses have been raised [49–51]. One further experiment, CoGeNT [6], reports the measurement of an yearly modulated signal. If interpreted in terms of a coherently interacting dark matter particle, this signal gives a region in the $m_\chi - \xi\sigma_{\rm scalar}^{\rm (nucleon)}$ plane, which is approximately located around $m_\chi \sim 10$ GeV and $\xi\sigma_{\rm scalar}^{\rm (nucleon)} \sim (3-10)\times 10^{-41}$ cm^2, thus somewhat displaced from the region singled out by the scatter plot of Fig. 6. However, a redetermination of the region toward smaller $\sigma_{\rm scalar}^{\rm (nucleon)}$ and larger m_χ is being undertaken by the CoGeNT Collaboration [52].

B. The neutralino subpopulation singled out by a Higgs at 126 GeV

We turn now to the analysis of a subset of the neutralino population considered in the previous section which would be selected by an indication of a possible Higgs signal at the LHC. Actually, the ATLAS Collaboration, in a search for a SM Higgs boson, measures an excess of events around a mass of 126 GeV, and restricts the most likely mass region (95% C.L.) to 115.5–131 GeV (global statistical significance about 2.3σ) [11]. Similar results (with a lower statistical significance) are presented by CMS [12]. We address the question of what might be the implications of these measurements (in case the effect is confirmed in future runs at the LHC) under the hypothesis that this possible signal is attributed to the production of the heavier neutral CP-even Higgs boson H of the MSSM [53].

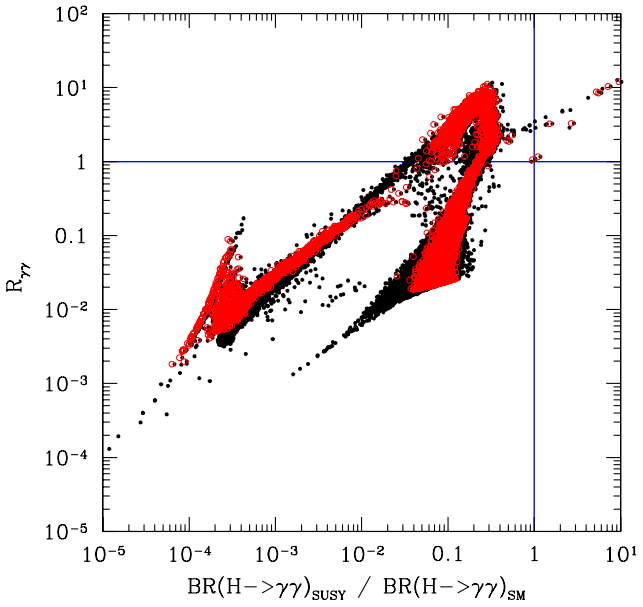

FIG. 6 (color online). Production cross-section ratio $R_{\gamma\gamma} \equiv [\sigma(gg \to H)\times {\rm BR}(H\to\gamma\gamma)]_{\rm MSSM}/[\sigma(gg\to h){\rm BR}(h\to\gamma\gamma)]_{\rm SM}$ as a function of ${\rm BR}(H\to\gamma\gamma)_{\rm MSSM}/{\rm BR}(h\to\gamma\gamma)_{\rm SM}$ for the configurations discussed in Sec. III A. Black points refer to H masses in the range 115 GeV $\le m_H \le$ 131 GeV, while (red) circles refer to an H mass interval more focused around 126 GeV (specifically: 125 GeV $\le m_H \le$ 127 GeV).

Within our light neutralino population, we select the subset of configurations with 115 GeV $\le M_H \le$ 131 GeV. These are contained in the band shown in the right panel of Fig. 2, with values of the m_A parameter in the range 90 GeV $\le M_A \le$ 129 GeV. This subpopulation of light neutralinos would have a neutralino-nucleon elastic cross section in the domain depicted in Fig. 5 by (red) crosses, and would then be in amazing agreement with the results of DM direct detection.

The identification of a putative Higgs boson with the H boson appears to be compatible in terms of production cross section and branching ratios. This is shown in Fig. 6, where the exclusive production cross-section ratio $R_{\gamma\gamma} \equiv [\sigma(gg\to H)\times{\rm BR}(H\to\gamma\gamma)]_{\rm MSSM}/[\sigma(gg\to H)\,{\rm BR}(H\to\gamma\gamma)]_{\rm SM}$ is plotted as a function of ${\rm BR}(H\to\gamma\gamma)_{\rm MSSM}/{\rm BR}(H\to\gamma\gamma)_{\rm SM}$ for our configurations. Here, $\sigma(gg\to H)$ is the Higgs production cross section through the gluon fusion process. We have calculated both quantities using FeynHiggs 2.8.6 [54]. Indeed, our population of light neutralinos contains many configurations which are in agreement with the putative Higgs signal. This is a property arising spontaneously in our scenario. Notice that although the BR of Higgs decay into 2 photons is typically smaller than the corresponding SM branchng ratio, $R_{\gamma\gamma}$ can be SM-like, due to enhanced production cross sections.

Though imposing the above requirement would imply some further selection within the neutralino population

previously discussed, we do not find in our scan any significant correlation between $R_{\gamma\gamma}$ and the properties of relic neutralinos, such as the neutralino relic abundance $\Omega_\chi h^2$ or the neutralino-nucleon cross section $\xi\sigma_{\text{scalar}}^{(\text{nucleon})}$. In fact $R_{\gamma\gamma}$ is mainly affected by the production cross section $\sigma(gg \to H)$, which depends on supersymmetric-QCD parameters that do not enter directly into the calculation of relic neutralino observables. Although a thorough analysis of these aspects is beyond the scope of the present paper, the previous considerations are sufficient to conclude that our scenario can be compatible with the possible Higgs signal at the LHC in a natural way.

IV. CONCLUSIONS

We have reviewed the status of the phenomenology of light neutralinos in an effective MSSM at the electroweak scale, in light of new results obtained at the CERN Large Hadron Collider. First, we considered the impact of the new data obtained by the CMS Collaboration on the search for the Higgs-boson decay into a tau pair, and by the CMS and LHCb Collaborations on the branching ratio for the decay $B_s \to \mu^+ + \mu^-$, and we established that, on the basis of these data, the new value for the lower bound of the neutralino mass is $m_\chi \simeq 18$ GeV.

Then, we have examined the possible implications of the excess of events found by the ATLAS and CMS Collaborations in a search for a SM-like Higgs boson around a mass of 126 GeV, with a most likely mass region (95% C.L.) restricted to 115.5–131 GeV (global statistical significance about 2.3σ). We have derived that the excess around $m_H^{\text{SM}} = 126$ GeV, which nevertheless needs a confirmation by further runs at the LHC, would imply a neutralino in the mass range $18\ \text{GeV} \lesssim m_\chi \lesssim 38\ \text{GeV}$, with neutralino-nucleon elastic cross sections fitting well the results of the dark matter direct search experiments DAMA/LIBRA and CRESST.

It is worth stressing that light neutralinos in the mass range considered here do not appear to be constrained by DM indirect searches (such as astrophysical gamma fluxes of diffuse extragalactic origin or from dwarf galaxies, and the low-energy cosmic antiproton flux). A detailed investigation of these aspects would however deserve a dedicated analysis.

ACKNOWLEDGMENTS

A. B. and N. F. acknowledge research grants funded jointly by Ministero dell'Istruzione, dell'Università e della Ricerca (MIUR), by Università di Torino, and by Istituto Nazionale di Fisica Nucleare within the *Astroparticle Physics Project* (MIUR Contract No. PRIN 2008NR3EBK; INFN Grant No. FA51). S. S. acknowledges support by the National Research Foundation of Korea (NRF) with a grant funded by the Korea government (MEST) Grant No. 2011-0024836. N. F. acknowledges support of the spanish MICINN Consolider Ingenio 2010 Programme under Grant No. MULTIDARK CSD2009-00064.

Note Added.—After the submission of the present paper, a new upper bound (at 95% C.L.) on the branching ratio for the decay $B_s \to \mu^+ + \mu^-$ has been presented by the LHCb Collaboration: $\text{BR}(B_s \to \mu^+\mu^-) < 4.5 \times 10^{-9}$ [56]. If the previous upper bound $\text{BR}(B_s \to \mu^+\mu^-) < 1.08 \times 10^{-8}$, employed in our analysis, is replaced by the new LHCb upper limit, the lower bound on the neutralino mass rises from the value of about 18 GeV, presented above, to about 20 GeV.

[1] A. Bottino, N. Fornengo, and S. Scopel, Phys. Rev. D **67**, 063519 (2003); **68**, 043506 (2003).
[2] A. Bottino, F. Donato, N. Fornengo, and S. Scopel, Phys. Rev. D **78**, 083520 (2008).
[3] N. Fornengo, S. Scopel, and A. Bottino, Phys. Rev. D **83**, 015001 (2011).
[4] R. Bernabei *et al.*, Riv. Nuovo Cimento **26N1**, 1 (2003).
[5] R. Bernabei *et al.*, Eur. Phys. J. C **67**, 39 (2010).
[6] C. E. Aalseth *et al.* (CoGeNT Collaboration), Phys. Rev. Lett. **106**, 131301 (2011); **107**, 141301 (2011).
[7] G. Angloher *et al.*, arXiv:1109.0702.
[8] Z. Ahmed *et al.* (CDMS Collaboration), Science **327**, 1619 (2010).
[9] A. Bottino, F. Donato, N. Fornengo, and S. Scopel, Phys. Rev. D **81**, 107302 (2010).
[10] P. Belli, R. Bernabei, A. Bottino, F. Cappella, R. Cerulli, N. Fornengo, and S. Scopel, Phys. Rev. D **84**, 055014 (2011).
[11] ATLAS Collaboration, Report No. ATLAS-CONF-2011-163.
[12] CMS Collaboration, Report No. report CMS PAS HIG-11-032.
[13] S. Scopel, S. Choi, N. Fornengo, and A. Bottino, Phys. Rev. D **83**, 095016 (2011).
[14] A. Bottino, N. Fornengo, and S. Scopel, Nucl. Phys. **B608**, 461 (2001).
[15] J. Dunkley *et al.* (WMAP Collaboration), Astrophys. J. Suppl. Ser. **180**, 306 (2009).
[16] A. Bottino, F. Donato, N. Fornengo, and S. Scopel, Astropart. Phys. **13**, 215 (2000); **18**, 205 (2002).
[17] S. Dinter, V. Drach, and K. Jansen, Int. J. Mod. Phys. E **20**, 110 (2011).
[18] J. M. Alarcon, J. Martin Camalich, and J. A. Oller, Phys. Rev. D **85**, 051503 (2012); J. Martin Camalich, J. M. Alarcón, and J. A. Oller, Prog. Part. Nucl. Phys. **67**, 327 (2012).

[19] J. R. Ellis, A. Ferstel, and K. A. Olive, Phys. Lett. B **481**, 304 (2000).

[20] T. K. Gaisser, G. Steigman, and S. Tilav, Phys. Rev. D **34**, 2206 (1986).

[21] A. Colaleo (ALEPH Collaboration), in Proceedings of SUSY'01, Dubna, Russia, 2001 (unpublished).J. Abdallah *et al.* (DELPHI Collaboration), Report No. DELPHI 2001-085 CONF 513, 2001; LEP Higgs Working Group for Higgs boson searches, arXiv:hep-ex/0107029; LEP2 Joint SUSY Working Group, http://lepsusy.web.cern.ch/lepsusy/.

[22] ALEPH, DELPHI, L3, OPAL, SLD, LEP Electroweak Working Group, SLD Electroweak Group, and SLD Heavy Flavour Group Collaborations, Phys. Rep. **427**, 257 (2006).

[23] K. Nakamura *et al.* (Particle Data Group), J. Phys. G **37**, 075021 (2010).

[24] E. Barberio *et al.* (HFAG), arXiv:hep-ex/0603003.

[25] M. Ciuchini, G. Degrassi, P. Gambino, and G. F. Giudice, Nucl. Phys. **B534**, 3 (1998).

[26] M. Misiak *et al.*, Phys. Rev. Lett. **98**, 022002 (2007).

[27] G. W. Bennet *et al.* (Muon $g-2$ Collaboration), Phys. Rev. D **73**, 072003 (2006).

[28] M. Davier, A. Hoecker, B. Malaescu, C. Z. Yuan, and Z. Zhang, Eur. Phys. J. C **66**, 1 (2010).

[29] T. Moroi, Phys. Rev. D **53**, 6565 (1996); **56**, 4424(E) (1997).

[30] V. Abazov *et al.* (D0 Collaboration), Phys. Lett. B **682**, 278 (2009).

[31] CMS Collaboration and LHCb Collaboration, Report Nos. LHCb-CONF-2011-047 and CMS PAS BPH-11-019.

[32] T. Aaltonen *et al.* (CDF Collaboration), Phys. Rev. Lett. **107**, 239903 (2011); Phys. Rev. Lett. **107**, 191801 (2011).

[33] R. Aaij *et al.* (LHCb Collaboration), Phys. Lett. B **708**, 55 (2012).

[34] A. J. Buras, P. H. Chankowski, J. Rosiek, and L. Slawianowska, Phys. Lett. B **546**, 96 (2002).

[35] G. Isidori and P. Paradisi, Phys. Lett. B **639**, 499 (2006).

[36] K. Nakamura, G. Bernardi, M. Carena, T. Junk *et al.* (Particle Data Group), J. Phys. G **37**, 075021 (2010).

[37] The CMS Collaboration, Report No. CMS PAS HIG-11-020.

[38] The CMS Collaboration, Report No. report CMS PAS HIG-11-029.

[39] J. Baglio and A. Djouadi, arXiv:1103.6247.

[40] J. Baglio, arXiv:1111.1195.

[41] H. K. Dreiner, S. Heinemeyer, O. Kittel, U. Langenfeld, A. M. Weber, G. Weiglein, Eur. Phys. J. C **62**, 547 (2009).

[42] A. Bottino, N. Fornengo, G. Polesello, and S. Scopel, Phys. Rev. D **77**, 115026 (2008).

[43] S. Choi, S. Scopel, N. Fornengo, and A. Bottino, Phys. Rev. D **85**, 035009 (2012).

[44] J. A. Conley, H. K. Dreiner, and P. Wienemann, Phys. Rev. D **83**, 055018 (2011).

[45] P. Belli, R. Bernabei, A. Bottino, F. Donato, N. Fornengo, D. Prosperi, and S. Scopel, Phys. Rev. D **61**, 023512 (1999).

[46] E. Aprile *et al.* (XENON100 Collaboration), Phys. Rev. Lett. **107**, 131302 (2011).

[47] D. S. Akerib *et al.* (CDMS Collaboration), Phys. Rev. D **82**, 122004 (2010); Z. Ahmed *et al.*, Phys. Rev. Lett. **106**, 131302 (2011).

[48] Sun Kee Kim (KIMS Collaboration), in Proceedings of TAUP 2011 [http://taup2011.mpp.mpg.de/?pg=Agenda].

[49] R. Bernabei, P. Belli, A. Incicchitti, and D. Prosperi, arXiv:0806.0011.

[50] J. I. Collar, arXiv:1106.0653.

[51] J. I. Collar, arXiv:1103.3481.

[52] J. I. Collar, in Proceedings of TAUP 2011 [http://taup2011.mpp.mpg.de/?pg=Agenda].

[53] This option is also entertained in S. Heinemeyer, O. Stal, and G. Weiglein, Phys. Lett. B **710**, 201 (2012).

[54] G. Degrassi, S. Heinemeyer, W. Hollik, P. Slavich, and G. Weiglein, Eur. Phys. J. C **28**, 133 (2003); S. Heinemeyer, W. Hollik, and G. Weiglein, Eur. Phys. J. C **9**, 343 (1999); Comput. Phys. Commun. **124**, 76 (2000).

[55] V. I. Tretyak, Astropart. Phys. **33**, 40 (2010).

[56] LHCb Collaboration, arXiv:1203.4493.